RSC Advances

PAPER

View Article Online
View Journal | View Issue

Cite this: *RSC Adv.*, 2019, **9**, 33519

$NaYF_4$:Yb,Tm@TiO_2 core@shell structures for optimal photocatalytic degradation of ciprofloxacin in the aquatic environment†

Yongmei Ma and Siyue Li*

Received 8th October 2019
Accepted 11th October 2019

DOI: 10.1039/c9ra08145c

rsc.li/rsc-advances

The removal of antibiotic residues in the aquatic environment is still a big challenge in environmental protection. Here, we developed $NaYF_4$:Yb,Tm@TiO_2 as a highly efficient photocatalyst for photocatalytic degradation of ciprofloxacin (CIP), a representative antibiotic in water under simulated solar irradiation. $NaYF_4$:Yb,Tm@TiO_2 can efficiently utilize a broad spectrum of solar energy to improve the efficiency of ciprofloxacin removal from an aquatic environment. The optimum operation conditions of photocatalyst dosage, pH value, and initial concentrations of CIP were determined by a series of contrast experiments. The dynamic process of CIP removal was monitored by UV-vis spectrophotometry, and can be well predicted by a pseudo first order model. The optimal conditions of photocatalyst dosage, initial concentration of CIP and pH value for CIP photocatalytic degradation were 1 g L^{-1}, 10^{-5} M and 8, respectively. This study provides an efficient method for antibiotic removal and enables a promising strategy for other organic water pollutant treatments.

Introduction

The widespread use of antibiotics in humans, animals and aquaculture results in vast residuals in aquatic environments.[1,2] The persistence of antibiotic residues may cause a series of problems in ecosystems and public health because of the poor biodegradability of antibiotics.[3] Therefore, the removal of antibiotic residues in aquatic environments is of great concern in environmental protection. In this case, many methods have been developed to deal with antibiotic residues, such as advanced oxidation treatment,[4] membrane treatments,[5] adsorption technology[6] and photoelectron-Fenton reactions.[7] However, most of these methods are costly and time-consuming. Also, some technologies need professionals to operate them. Therefore, it is still a challenge to develop an environmentally friendly, simple and efficient approach to remove antibiotic residues from aquatic environments.

Photocatalytic degradation technology has been considered as an effective and promising technology to remove antibiotic residues from water. Among the most photocatalysts, titanium dioxide (TiO_2) has aroused the increasing concern due to the extraordinary chemical stability, high photocatalytic activity, biocompatible features, low cost, wide application and environmental friendliness.[8–10] However, the photons absorption capacity of TiO_2 is poor due to the broad band gap of *ca.* 3.2 eV, which requires ultraviolet (UV) light activation.[11] UV light accounts for only 5% of sunlight,[12] which limits the application of TiO_2 in environment restoration. Effort therefore have been focused on extending the range of absorption wavelength of TiO_2 to the visible or even NIR region for improving the photocatalytic efficiency.[13–15] The TiO_2 absorption wavelength rang can be extended by numerous reformative methods, such as metals and nonmetallic ions doping, cationic substitutions, anionic doping, and so on.[16–18] However, most of these methods suffer from expensive requirement, complex treated process and overall catalytic capability decreasing.[19,20] Therefore, it remains an urgent problem to improve the photons absorption and photocatalytic capacity of TiO_2 at the same time.

Different from the traditional methods to extend the absorption of TiO_2, a promising strategy is transferring visible and near infrared lights into UV lights, which can activate TiO_2 particles better and improve photocatalytic efficiency. Upconversion (UC) materials have attracted much attention due to the special property of transferring NIR light into visible and UV light.[21,22] It is an effective method to introduce UC materials to photocatalysts, which can improve the photocatalytic efficiency and utilization efficiency of sunlight. The hybrid structure of UC and UV-active photocatalysts had been synthesized, and used for environmental conservation.[23–25] In our earlier work, we have prepared composite photocatalyst ($NaYF_4$:Yb,Tm@TiO_2/Ag) which has the good photocatalytic function for organic pollutants degradation under Xe lamp irradiation.[26] However, that report did not research the optimization conditions of the composite photocatalyst to remove organic pollutants, such as

Research Center for Ecohydrology, Chongqing Institute of Green and Intelligent Technology, Chinese Academy of Sciences, Chongqing 400714, China. E-mail: syli2006@163.com; Fax: +86 23 65935000; Tel: +86 23 65935058

† Electronic supplementary information (ESI) available: figure and tables. See DOI: 10.1039/c9ra08145c

the concentration of organic pollutants, photocatalyst dosage and pH value. It is essential to optimize these parameters, which would affect the organic pollutants removal in practical application. May For example, (i) the concentration of organic pollutants in water can influence their contact with photocatalysts; (ii) the light penetration can be influenced by photocatalyst dosage;[27] (iii) the pH value of solution can also influence the contact between organic pollutants and photocatalyst.[28,29]

In this study, ciprofloxacin (CIP), a common fluoroquinolone antibiotic, was employed to explore the optimum operation conditions of $NaYF_4$:Yb,Tm@TiO_2 for antibiotic residues removal and its photocatalytic degradation mechanism. The optimized operation conditions of photocatalyst dosage, pH value, and initial concentrations of CIP were determined by a series of contrast experiments. The dynamic process of CIP removal by $NaYF_4$:Yb,Tm@TiO_2 under Xe lamp was monitored by UV-vis spectrophotometer to evaluate its photocatalytic efficiency. These results indicated that this photocatalytic platform can efficiently remove various organic pollutants in aquatic environments. The original contribution of this study was that we obtained the optimum operation conditions to effectively remove the CIP by $NaYF_4$:Yb,Tm@TiO_2 under Xe lamp and the possible mechanism of this reaction.

Experimental section

Chemicals and materials

Titanium *n*-butoxide ($Ti(OBu)_4$), sodium citrate, $TmCl_3$, NaF, $YbCl_3 \cdot 6H_2O$, and $YCl_3 \cdot 6H_2O$ were purchased from Shanghai Reagent Co., all the chemicals were analytical reagents grade and directly used without further treatment. The solutions were prepared by distilled water and no pH regulation. All experiments were conducted under room temperature (25 °C) in water systems.

Synthesis of $NaYF_4$:Yb,Tm@TiO_2

The $NaYF_4$:Yb, Tm@TiO_2 core@shell structures were prepared according to our earlier work.[26]

Photocatalytic experiments

CIP was used to evaluate the photocatalytic activities of the $NaYF_4$:Yb,Tm@TiO_2 under the irradiation of a Xe lamp (set at 200 W). In a typical process, the $NaYF_4$:Yb,Tm@TiO_2 particles were dispersed into CIP solution in a 100 mL quartz tube under different conditions, such as pH value, $NaYF_4$:Yb,Tm@TiO_2 dosage and the concentrations of CIP. 1 M HCl or NaOH solution was used to adjust the initial pH of CIP solution during the photocatalytic degradation process. To obtain the real initial of CIP solution before the photocatalytic degradation, the solution was stirred for 2 h in the dark to reach an adsorption–desorption equilibrium between $NaYF_4$:Yb,Tm@TiO_2 and CIP solution. Subsequently, the quartz tube was exposed to irradiation from a Xe lamp, 3 mL of CIP aqueous solution was intermittently collected at given time intervals for centrifugation. The filtrate was measured by UV-vis spectroscopy.

Apparatus

The scanning electron microscopy (SEM) images were recorded by a Sirion 200 field-emission scanning electron microscope. X-ray scattering patterns were taken by analyzing the powder samples on a Philips X-Pert Pro X-ray diffractometer (XRD) with Cu Kα radiation. A JEOL 2010 high resolution transmission electron microscope with X-ray energy dispersive spectroscopy capabilities was used to record transmission electron microscopy (TEM) images, and operated at an acceleration voltage of 200 kV. The UV-vis absorbance spectra of the CIP solution were measured by Lambda 35 UV-vis spectrometer (PerkinElmer, Waltham, MA, USA).

Results and discussion

Hexagonal prisms of $NaYF_4$:Yb,Tm with average side length about 400 nm were successfully synthesized (Fig. 1A–C). A straightforward method was developed to decorate TiO_2 on the surface of $NaYF_4$:Yb,Tm. Fig. 1D–F showed that all elements of Yb, Tm and Ti were distributed throughout the entire particle. More importantly, after coating TiO_2, the core@shell structure of $NaYF_4$:Yb,Tm@TiO_2 was clearly observed from SEM and TEM images (Fig. 1B and C).

The XRD pattern of $NaYF_4$:Yb,Tm (Fig. 2) was consistent with the standard values of hexagonal phase $NaYF_4$ crystals (JCPDS files no. 28-1192). The new peaks at $2\theta = 25.3°$, 38°, 48.1°, 55.4°, 62.9°, 68.9°, 75.2°, 83.2° in the curve of $NaYF_4$:Yb,Tm@TiO_2 were consistent with the standard values of anatase-phase TiO_2 (JCPDS files no. 21-1272). This result further evidenced the successful decorating of TiO_2 on the surface of $NaYF_4$:Yb,Tm.

In our previous work, we have proved that $NaYF_4$:Yb,Tm can convert NIR light into UV light to activate TiO_2 and induce the photocatalytic activity of $NaYF_4$:Yb,Tm@TiO_2 under NIR irradiation. This compound photocatalyst can efficiently utilize different bands of the solar spectrum, which enables a promising application in photocatalytic degradation of organic pollutant in water. For example, the capacity of TiO_2 for photocatalytic degradation antibiotic can be improved after introducing $NaYF_4$:Yb,Tm under Xe lamp irradiation (Fig. S1†). In

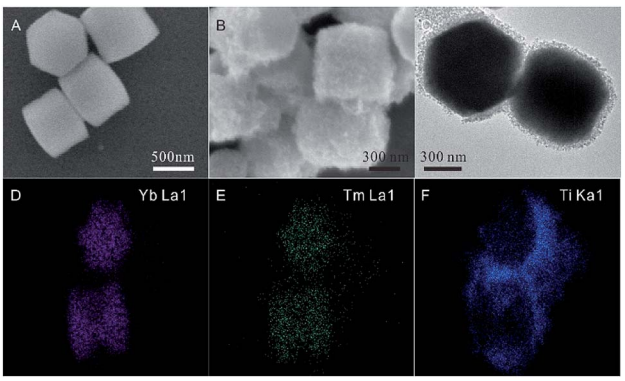

Fig. 1 (A) SEM image of $NaYF_4$:Yb,Tm. (B) SEM and (C) TEM images of $NaYF_4$:Yb,Tm@TiO_2. (D–F) Elemental mapping of $NaYF_4$:Yb,Tm@TiO_2 particles, including Yb La1, Tm La1 and Ti Ka1.

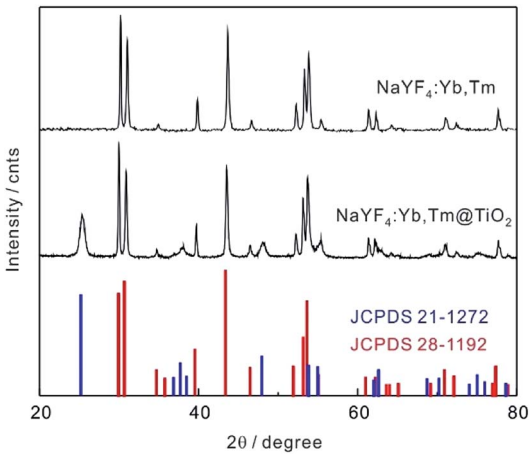

Fig. 2 XRD patterns of $NaYF_4$:Yb,Tm, $NaYF_4$:Yb,Tm@TiO_2 and standard XRD patterns of $NaYF_4$ (JCPDS 28-1192) and anatase-phase TiO_2 (21-1272).

order to maximize the photocatalytic efficiency of the photocatalyst under Xe lamp irradiation, CIP was used to study the optimization conditions of the composite photocatalyst for organic pollutants removal, including pH value, $NaYF_4$:Yb,Tm@TiO_2 dosage and the concentrations of CIP.

3 mL of CIP solution was taken out and centrifuged after irradiation a designated time by Xe lamp, and the supernatant was measured by UV-vis spectroscopy. The influence of $NaYF_4$:Yb,Tm@TiO_2 dosage on the efficiency of CIP removal has been shown in Fig. 3. Fig. 3A displayed the absorbance spectra of CIP (1×10^{-5} M) photocatalytic degraded by 1 g L^{-1} $NaYF_4$:Yb,Tm@TiO_2 under Xe lamp irradiation as a function of the irradiation time. As expected, the absorption intensity of CIP at 274 nm decreased with irradiation time increase, indicating the photocatalytic degradation of CIP under current

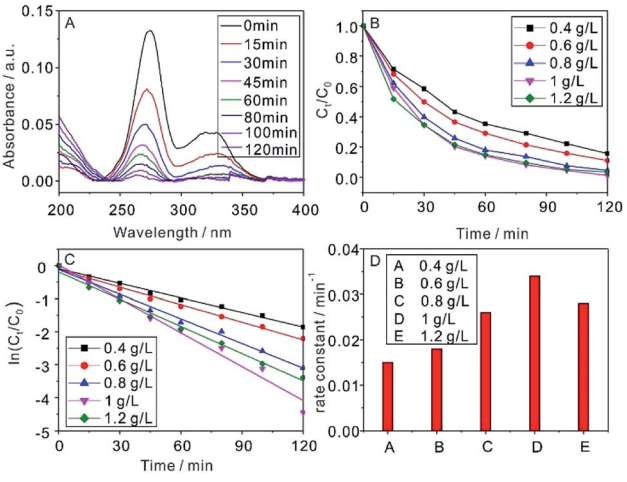

Fig. 3 (A) Time-course UV-vis absorbance spectra of CIP (10^{-5} M) photocatalyzed by 1 g L^{-1} $NaYF_4$:Yb,Tm@TiO_2 under Xe lamp. (B–D) The calculated time-dependent ratios of C/C_0, first-order degradation rates, and reaction rate constants under Xe lamp with different $NaYF_4$:Yb,Tm@TiO_2 dosage.

condition. The photocatalytic degradation activity of $NaYF_4$:Yb,Tm@TiO_2 was evaluated by comparing the filtrate concentration at each designated irradiation time to that at time zero. The photocatalytic degradation degree of CIP can be revealed by the plots of the time-dependent curves of the C_t/C_0 ratio (Fig. 3B). C_0 represent the initial concentration of CIP and C_t was the measured concentration of CIP at designated irradiation time t. C_t was obtained from comparing 274 nm absorbance intensity of CIP with that of standard CIP solution. After 2 h irradiation, about 75%, 89%, 96%, 99% and 97% of CIP were photocatalytic degraded under the $NaYF_4$:Yb,Tm@TiO_2 dosage of 0.4, 0.6, 0.8, 1 and 1.2 g L^{-1}, respectively. In order to further evaluate the influence of $NaYF_4$:Yb,Tm@TiO_2 dosage on the efficiency of CIP removal, Fig. 3C showed the kinetics of the photocatalytic degradation reactions, which can be described as pseudo first order by eqn (1).[26]

$$\ln\frac{C_t}{C_0} = -kt \quad (1)$$

The rate constants (k, min^{-1}) were evaluated from plots of $\ln(C_t/C_0)$ *vs.* irradiation time t. The calculated rate constants of 0.4, 0.6, 0.8, 1 and 1.2 g L^{-1} of $NaYF_4$:Yb,Tm@TiO_2 dosage were 0.015, 0.018, 0.026, 0.034 and 0.028, respectively (Fig. 3D and Table S1†). As the increasing of photocatalyst dosage, the best reaction rate constant can be obtained when $NaYF_4$:Yb,Tm@TiO_2 dosage was 1 g L^{-1}. After that, the reaction rate constant was decreased with increasing $NaYF_4$:Yb,Tm@TiO_2 dosage up to 1.2 g L^{-1}. The turbidity induced by more photocatalyst dosage lead to light scattering, which can reduce the capacity of light penetration into the solution and counteract the effect of photocatalyst surface area. Both of these caused the efficiency of photocatalyst decrease for CIP removal.[30] The R^2 of pseudo first order kinetic model for CIP removal with $NaYF_4$:Yb,Tm@TiO_2 dosage of 0.4, 0.6, 0.8, 1 and 1.2 g L^{-1} were 0.989, 0.991, 0.991, 0.978 and 0.991, respectively (Table S1†). The high R^2 values demonstrated the reasonable photocatalytic degradation kinetic experimental data handling based on the pseudo first order kinetic model.[31]

To further investigate the photocatalytic degradation capacity of the photocatalyst, different CIP concentrations were photocatalyzed with 1 g L^{-1} $NaYF_4$:Yb,Tm@TiO_2 under Xe lamp irradiation (Fig. 4). Fig. 4A showed the absorbance spectra of CIP (1×10^{-5} M) photocatalyzed by 1 g L^{-1} $NaYF_4$:Yb,Tm@TiO_2 under Xe lamp irradiation as a function of the reaction time. The time-dependent curves of C_t/C_0 ratio was shown in Fig. 4B. After 2 h irradiation, the concentrations of 10^{-5} and 5×10^{-6} M CIP had been almost photocatalytic degraded. Meanwhile, only 66% and 50% CIP solution were photocatalytic degraded when the concentrations were 2.5×10^{-5} and 5×10^{-5} M, respectively. The kinetics of the photocatalytic degradation reactions also can be described as pseudo first order according to eqn (1) (Fig. 4C). The evaluated rate constants with the CIP concentrations of 5×10^{-5}, 2.5×10^{-5}, 10^{-5} and 5×10^{-6} M were 0.006, 0.009, 0.034 and 0.034, respectively (Fig. 4D and Table S2†). These results showed that the rate constant didn't increase when the concentration of CIP exceed 10^{-5} M under current

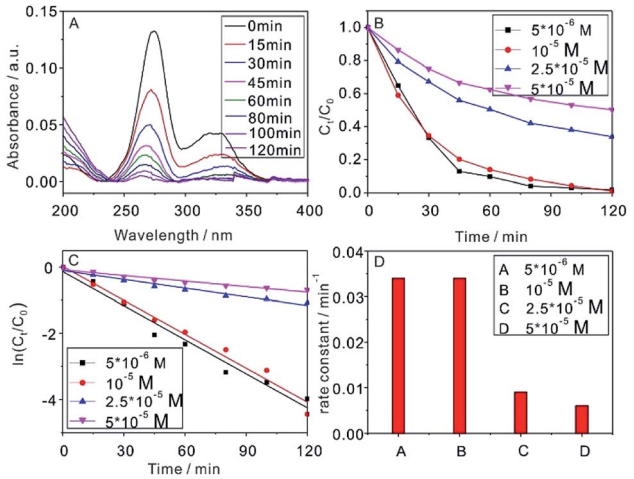

Fig. 4 (A) Time-course UV-vis absorbance spectra of CIP (10^{-5} M) photocatalyzed by 1 g L^{-1} $NaYF_4$:Yb,Tm@TiO_2 under Xe lamp. (B–D) The calculated time-dependent ratios of C/C_0, first-order degradation rates, and reaction rate constants for different concentration of CIP photocatalyzed by 1 g L^{-1} $NaYF_4$:Yb,Tm@TiO_2 under Xe lamp.

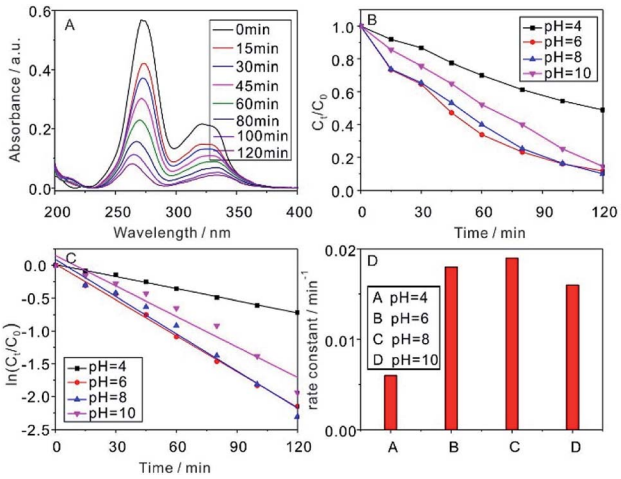

Fig. 5 (A) Time-course UV-vis absorbance spectra of CIP (10^{-5} M) photocatalyzed by 1 g L^{-1} $NaYF_4$:Yb,Tm@TiO_2 under Xe lamp at pH = 8. (B–D) The calculated time-dependent ratios of C/C_0, first-order degradation rates and reaction rate constants for CIP (10^{-5} M) photocatalyzed 1 g L^{-1} $NaYF_4$:Yb,Tm@TiO_2 with different pH values.

conditions. Generally speaking, the reaction rate constant will increase with the pollutants concentration decrease. However, the capacity of the photocatalyst may not show efficiently when less pollutants reached to photocatalyst surface due to the low concentration. Thus, the choosing concentration of CIP in next experiments was 10^{-5} M. The R^2 of pseudo first order kinetic model for CIP removal with the concentrations of 5×10^{-5}, 2.5×10^{-5}, 10^{-5} and 5×10^{-6} M were 0.969, 0.978, 0.963 and 0.937, respectively (Table S2†). The high R^2 values also demonstrated the reasonable photocatalytic degradation kinetic experimental data handling based on the pseudo first order kinetic model.

The solubility and lipophilicity of CIP are pH-dependent, because it has carboxylic acid group (pK_{a1} = 6.1) and an amine group in the piperazine moiety (pK_{a2} = 8.7).[32] Therefore, the initial pH of the aqueous solution is a significant parameter in photocatalytic degradation process, which influences the activity and stability of photocatalyst and further influence the efficiency of CIP removal.[33] Fig. 5 showed the actual influence of pH on the efficiency of CIP removal by $NaYF_4$:Yb,Tm@TiO_2 under Xe lamp irradiation. Fig. 5A displayed the absorbance spectra of CIP (1×10^{-5} M) photocatalyzed by 1 g L^{-1} $NaYF_4$:Yb,Tm@TiO_2 at pH = 8 under Xe lamp irradiation as a function of the reaction time. Fig. 5B showed the time-dependent curves of C_t/C_0 ratio and indicate the photocatalytic activity of $NaYF_4$:Yb,Tm@TiO_2. After 2 h irradiation, about 51%, 88%, 90% and 85% of CIP solution was photocatalytic degraded at pH = 4, 6, 8 and 10, respectively. According to eqn (1), the reaction rate constants were derived from the linearly fitted slope (Fig. 5C). The calculated values of rate constants at pH = 4, 6, 8 and 10 were 0.006, 0.018, 0.019 and 0.016, respectively (Fig. 5D and Table S3†). The results indicated that the biggest value of reaction rate constant was obtained at pH = 8. Under acidic conditions, the CIP molecule has positive charge because of protonization of the pyrazine ring. Under alkaline conditions, the CIP molecule exists as a monovalent anion (CIP–COO^-) because of deprotonation of a carboxyl group. CIP and photocatalyst surface have the same charge both acidic and alkaline conditions, and the electrostatic repulsion force will hinder CIP molecule to the surface of photocatalyst.[34,35] Therefore, in this study, when pH value is less than 8, rate constants increased with pH increase; however, when pH value is more than 8, rate constants decreased with pH increase. Under neutral conditions, the CIP molecule exists as the zwitterion, showing the lowest solubility and the highest hydrophobicity. And the hydrophobic interactions can promote more and more CIP molecule to reach the surface of photocatalyst.[32] The photocatalytic degradation capacities of CIP peaked at pH = 8 in the research data. Actually, the neutral conditions were a better choice for this reaction. The R^2 of pseudo first order kinetic model for CIP removal at pH = 4, 6, 8 and 10 were 0.997, 0.995, 0.981 and 0.946, respectively (Table S3†). The high R^2 values also demonstrated the reasonable photocatalytic degradation kinetic experimental data handling based on the pseudo first order kinetic model.

In view of the fact that $NaYF_4$:Yb,Tm can convert NIR light to UV light and further activate TiO_2 particles, the mechanism of CIP photocatalytic degradation by $NaYF_4$:Yb,Tm@TiO_2 under Xe lamp irradiation was elucidated and shown in Scheme 1. Under the irradiation of Xe lamp, TiO_2 absorbed UV light converted by $NaYF_4$:Yb,Tm, and excited electrons from valence band (CB) to conduction band (VB), creating electron–hole pairs.[36] The electron–hole pairs will migrate to the surface of photocatalyst and take part in photocatalytic reactions. The excited electrons can react with the oxygen to form superoxide $^{\bullet}O^{2-}$ radical anions, and then react with H^+ to form hydroxyl radicals ($^{\bullet}OH$) at last. At the same time, holes can react with H_2O to form $^{\bullet}OH$.[37,38] The organic pollutant molecules will react with these oxidizing agents and then photocatalytic degraded by the oxidizing agents. Because of the strong oxidizing power of $^{\bullet}OH$, most of the organics will be oxidized finally to CO_2 and H_2O.

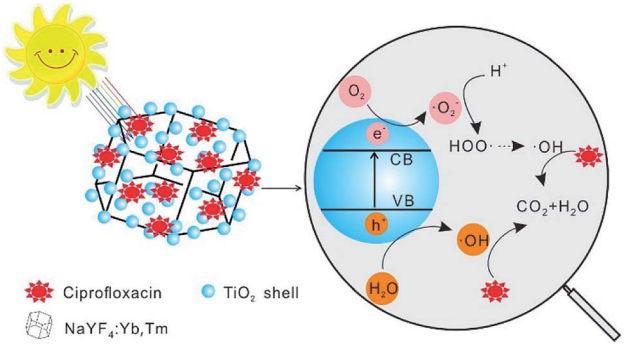

Scheme 1 Illustrated mechanism of photocatalytic degradation of CIP on $NaYF_4$:Yb,Tm@TiO_2 under Xe lamp irradiation.

Conclusions

In summary, $NaYF_4$:Yb,Tm@TiO_2 has been used as a highly efficient photocatalyst for photocatalytic degradation of ciprofloxacin in wastewater under Xe lamp irradiation. The kinetics of photocatalytic degradation reaction was monitored by UV spectroscopy, and simulated by pseudo first order model with suitable degrees of fitting. The influences of photocatalyst dosage, concentration of MG and pH values to the efficiency of CIP removal were investigated by analyzing the kinetics of photocatalytic reaction. 1 g L^{-1}, 10^{-5} M and 8 were the optimal value of photocatalyst dosage, initial concentrations of CIP and pH, respectively to obtained the maximum efficiency of CIP degradation. This photocatalyst can efficiently utilize different range of solar energy, which improves its application in the field of water treatment, and enables a promising strategy to investigate the photocatalytic degradation of antibiotic.

Conflicts of interest

The authors declare no competing financial interests.

Acknowledgements

This study was financially supported by the National Natural Science Foundation of China (NSFC 21806164) and West Light Foundation of the Chinese Academy of Sciences (granted to Dr Yongmei Ma).

Notes and references

1 X. J. Wen, C. G. Niu, L. Zhang, C. Liang and G. M. Zeng, *Appl. Catal., B*, 2018, **221**, 701–714.
2 P. C. Pinheiro, S. Fateixa, H. I. S. Nogueira and T. Trindade, *Nanomaterials*, 2019, **9**, 31–49.
3 T. S. Anirudhan, F. Shainy and J. Christa, *J. Hazard. Mater.*, 2017, **324**, 117–130.
4 C. L. Jiang, Y. F. Ji, Y. Y. Shi, J. F. Chen and T. M. Cai, *Water Res.*, 2016, **106**, 507–517.
5 V. Homem and L. Santos, *J. Environ. Manage.*, 2011, **92**, 2304–2347.
6 L. Liu, Q. F. Deng, T. Y. Ma, X. Z. Lin, X. X. Hou, Y. P. Liu and Z. Y. Yuan, *J. Mater. Chem.*, 2011, **21**, 16001–16009.
7 E. Guinea, J. A. Garrido, R. M. Rodriguez, P. L. Cabot, C. Arias, F. Centellas and E. Brillas, *Electrochim. Acta*, 2010, **55**, 2101–2115.
8 S. D. Zhao, J. R. Chen, Y. F. Liu, Y. Jiang, C. G. Jiang, Z. L. Yin, Y. G. Xiao and S. S. Cao, *Chem. Eng. J.*, 2019, **367**, 249–259.
9 S. H. Qin, W. Y. Cai, X. H. Tang and L. B. Yang, *Analyst*, 2014, **139**, 5509–5515.
10 Y. Jin, D. L. Jiang, D. Li and M. Chen, *Catal.: Sci. Technol.*, 2017, **7**, 2308–2317.
11 J. Wang, G. Zhang, Z. H. Zhang, X. D. Zhang, G. Zhao, F. Y. Wen, Z. J. Pan, Y. Li, P. Zhang and P. L. Kang, *Water Res.*, 2006, **40**, 2143–2150.
12 Y. N. Tang, W. H. Di, X. S. Zhai, R. Y. Yang and W. P. Qin, *ACS Catal.*, 2013, **3**, 405–412.
13 Y. Shiraishi, H. Sakamoto, K. Fujiwara, S. Ichikawa and T. Hirai, *ACS Catal.*, 2014, **4**, 2418–2425.
14 D. Kim, B. C. Yeo, D. Shin, H. Choi, S. Kim, N. Park and S. S. Han, *Phys. Rev. B*, 2017, **95**, 045209.
15 L. Yang, Y. An, B. Dai, X. H. Guo, Z. Y. Liu and B. H. Peng, *Korean J. Chem. Eng.*, 2017, **34**, 476–483.
16 Z. G. Xiong and X. S. Zhao, *J. Am. Chem. Soc.*, 2012, **134**, 5754–5757.
17 A. Yu, Q. J. Wang, J. J. Wang and C. T. Chang, *Catal. Commun.*, 2017, **90**, 75–78.
18 K. L. Chow, Y. B. Man, N. F. Y. Tam, Y. Liang and M. H. Wong, *J. Hazard. Mater.*, 2017, **322**, 263–269.
19 L. Xu, E. M. P. Steinmiller and S. E. Skrabalak, *J. Phys. Chem. C*, 2012, **116**, 871–877.
20 H. Y. Chuang and D. H. Chen, *Nanotechnology*, 2009, **20**, 105704.
21 F. Auzel, *Chem. Rev.*, 2004, **104**, 139–173.
22 J. Zhou, Q. Liu, W. Feng, Y. Sun and F. Y. Li, *Chem. Rev.*, 2015, **115**, 395–465.
23 A. Kumar, K. L. Reddy, S. Kumar, A. Kumar, V. Sharma and V. Krishnan, *Acs Appl. Mater. Inter.*, 2018, **10**, 15565–15581.
24 H. N. Huang, Z. Y. Wang, B. B. Huang, P. Wang, X. Y. Zhang, X. Y. Qin, Y. Dai, G. J. Zhou and M. H. Whangbo, *Adv. Opt. Mater.*, 2018, **6**, 1701331.
25 W. Wang, M. Y. Ding, C. H. Lu, Y. R. Ni and Z. Z. Xu, *Appl. Catal., B*, 2014, **144**, 379–385.
26 Y. M. Ma, H. L. Liu, Z. Z. Han, L. B. Yang and J. H. Liu, *J. Mater. Chem. A*, 2015, **3**, 14642–14650.
27 X. H. Huang, M. Leal and Q. L. Li, *Water Res.*, 2008, **42**, 1142–1150.
28 X. D. Wang and R. A. Caruso, *J. Mater. Chem.*, 2011, **21**, 20–28.
29 A. Mills and S. LeHunte, *J. Photochem. Photobiol., A*, 1997, **108**, 1–35.
30 J. K. Yang and S. M. Lee, *Chemosphere*, 2006, **63**, 1677–1684.
31 B. S. Zhu, Y. Jia, Z. Jin, B. Sun, T. Luo, X. Y. Yu, L. T. Kong, X. J. Huang and J. H. Liu, *Chem. Eng. J.*, 2015, **271**, 240–251.
32 H. B. Li, D. Zhang, X. Z. Han and B. S. Xing, *Chemosphere*, 2014, **95**, 150–155.

33 S. B. Wu, K. S. Zhang, X. L. Wang, Y. Jia, B. Sun, T. Luo, F. L. Meng, Z. Jin, D. Y. Lin, W. Shen, L. T. Kong and J. H. Liu, *Chem. Eng. J.*, 2015, **262**, 1292–1302.
34 H. B. Li, W. H. Wu, X. X. Hao, S. Wang, M. Y. You, X. Z. Han, Q. Zhao and B. S. Xing, *Environ. Pollut.*, 2018, **243**, 206–217.
35 H. Fu, X. B. Li, J. Wang, P. F. Lin, C. Chen, X. J. Zhang and I. H. Suffet, *J. Environ. Sci.*, 2017, **56**, 145–152.
36 X. H. Li, G. Y. Chen, L. B. Yang, Z. Jin and J. H. Liu, *Adv. Funct. Mater.*, 2010, **20**, 2815–2824.
37 S. Furukawa, T. Shishido, K. Teramura and T. Tanaka, *ACS Catal*, 2012, **2**, 175–179.
38 D. S. Muggli, J. T. McCue and J. L. Falconer, *J. Catal.*, 1998, **173**, 470–483.